A highly porous type II collagen containing scaffold for the treatment of cartilage defects enhances MSC chondrogenesis and early cartilaginous matrix deposition.

Claudio Intini[1,2], Mark Lemoine[1,2], Tom Hodgkinson[1,2], Sarah Casey[1,2], John P. Gleeson[1,3,*] & Fergal J. O'Brien[1,2,4,*].

[1]Tissue Engineering Research Group, Department of Anatomy & Regenerative Medicine, Royal College of Surgeons in Ireland (RCSI), Dublin, Ireland. [2]Advanced Materials and Bioengineering Research (AMBER) Centre, RCSI & TCD. [3]Fraunhofer Project Centre for Embedded Bioanalytical Systems, Dublin City University, Glasnevin, Dublin 9, Ireland. [4]Trinity Centre for Biomedical Engineering, Trinity College Dublin (TCD), Dublin 2, Ireland.

*These authors share senior authorship.

Abstract

A major challenge in cartilage tissue engineering (TE) is the development of instructive and biomimetic scaffolds capable of driving effective mesenchymal stem cell (MSC) chondrogenic differentiation and robust *de novo* matrix formation. Type I collagen-based scaffolds are one of the most commonly selected materials given collagen's intrinsic ability to act as an instructive and active biomaterial. However, the chondrogenic potential of these scaffolds does not offer significant improvement over traditional treatments. We propose that taking a biomimetic approach to scaffold development might lead to an improved outcome for enhanced cartilage repair. Therefore, this study aimed to develop innovative type II collagen (CII)-containing scaffolds for enhanced cartilage repair, by incorporating CII and/or hyaluronic acid (HyA) into a type I collagen (CI) framework. Moreover, focus was placed on understanding the potential synergistic effects played by CII in combination with HyA, in terms of MSC chondrogenesis and cartilage-like formation, when both molecules are incorporated into scaffold biomaterials. The newly developed CII-containing scaffold exhibited a highly porous interconnected structure with 99% porosity and similar mechanical properties to previously optimised collagen-based scaffolds. Although all scaffold variants sustained early cartilaginous matrix deposition, the CII-containing scaffolds in the presence of HyA performed best, offering enhanced deposition and distribution of sulphated glycosaminoglycans (sGAG) *in vitro* by day 28. Taken together, the combination of CII and HyA resulted in the development of a biomimetic scaffold with improved chondrogenic

benefits. These simple “off-the-shelf” implants hold great promise to direct enhanced tissue regeneration for the treatment of focal cartilage defects.

1 Introduction

Biomimetic scaffold biomaterials, with compositon and structure based on the native extra cellular matrix, play a fundamental role in tissue engineering (TE) by providing essential three-dimensional (3D) cues for infiltrating cellular populations, such as mesenchymal stem cells (MSC), to generate a *de novo* engineered tissue[1,2]. In particular, the composition of these scaffolds can significantly impact MSC behaviour in terms of differentiation toward an accurate cellular phenotype, subsequently directing the type of engineered tissue formed[3]. A major challenge in cartilage TE is to develop scaffolds capable of providing an improved instructive and active response to drive effective MSC differentiation and robust *de novo* matrix formation while retaining the essential mechanical properties of the implant[1,4]. Collagen-based scaffolds are one of the most commonly selected starting materials as 3D biomimetic templates in cartilage TE[5,6]. Collagen possesses a number of major advantages being biodegradable and biocompatible, easily available, and highly versatile compared to other biologic or synthetic materials[2,5]. In addition, collagen can be an instructive and active biomaterial given the intrinsic functional groups within it’s structure which can facilitate cell-extracellular matrix (ECM) interactions[7,8,9]. Moreover, the incorporation of ECM components such as glycosaminoglycans (GAGs) within collagen-based scaffolds might significantly improve the responsiveness of MSCs to chondrogenic cues[10]. This is the approach taken in previous studies in our laboratory, whereby the incorporation of hyaluronic acid (HyA) (a fundamental non-sulphated GAG component within cartilage tissue) within type I collagen-based scaffolds improved early cartilage ECM deposition and distribution[10].

In cartilage, type II collagen (CII) is the main structural ECM component, forming a fibrillar collagen network which is connected to the extrafibrillar network via HyA[11,12]. This particular ECM arrangement, composed of CII in combination with HyA and sulphated GAGs, results in a well-structured supramolecular organisation which provides the fundamental mechanical properties of the tissue and allows it to resist compression during loading. In addition, previous research suggests CII is one of the key factors co-regulating the anabolic and catabolic processes within articular cartilage, particularly chondrocyte homeostasis[12,13,14]. A progressive lack of CII within the tissue appears to correlate with irreversible articular chondrocyte catabolic disorders, subsequently resulting in inferior quality tissue that is

mechanically incapable of sufficiently executing its normal functions[12]. From a TE perspective, the potential of CII to act as an instructive and bioactive biomaterial capable of modifying tissue homeostasis and cellular behaviours is of great interest. The incorporation of CII into two-/three-dimensional (2D/3D) biomimetic implants has revealed its capability to influence MSC behaviour, specifically promoting improved cellular responses towards cartilage-like matrix formation *in vitro*[15,16]. In particular, CII has shown some potential in enhancing the chondrogenic response in MSCs, by reducing cellular hypertrophic differentiation and subsequent further chondrogenic differentiation towards osteogenesis and endochondral bone formation[17,18,19]. Previous work in our laboratory has also led to the development of novel tri-layered osteochondral collagen-based scaffolds incorporating CII (in the articular cartilage layer), optimised for orthopaedic applications[20]. These patented tri-layered scaffolds consist of a first layer (for bone repair) composed of type I collagen and hydroxyapatite (CI-HA), an intermediate layer (corresponding to the deep zone of cartilage) made with type I collagen and hyaluronic acid (CI-HyA) and a superficial articular cartilage layer composed of type I/type II collagen and hyaluronic acid (CI/II- HyA). These tri-layered scaffolds have been shown to possess significant cartilage/bone regenerative capacity *in vivo* in both small and large animal models, as well as in a recent pilot study in humans[21,22,23]. However, the role played by CII and the mechanism by which it enhances cartilage-like formation within these biomaterials remains to be elucidated.

Building on this knowledge, the primary hypothesis of this study was that the incorporation of CII into type I collagen-based scaffolds would affect MSC behaviour leading to improved chondrogenesis and cartilage-like tissue formation *in vitro*. To this end, the porous type I collagen-based scaffolds scaffold incorporating CII were investigated: (1) for their architectural, morphological and mechanical properties, and (2) their capability to enhance the chondrogenic response in MSCs, that consequently results in improved cartilage-like tissue formation *in vitro*.

2 Materials and methods

2.1 Fabrication of collagen-based scaffolds

To fabricate the collagen-based scaffolds, a freeze-drying method (lyophilisation) previously described and regularly used in our research group was used[24]. Type I collagen (CI), hyaluronic acid (HyA) and type II collagen (CII) were used at various ratios to prepare a series of type I collagen-based scaffold iterations (Table 1). CI scaffolds were composed of

collagen derived from bovine achilles tendon (Collagen Matrix, USA). CI and HyA (CI-HyA) scaffolds were composed of CI and HyA sodium salt derived from *Streptococcus equi* (molecular weight 1500-1800 kDa) (Sigma-Aldrich, Ireland). Finally, combination CI/II scaffolds and CI/II-HyA scaffolds were manufactured by incorporating CII isolated from porcine knee cartilage (Symatese, France). Briefly, CI slurry was prepared by suspending 1.8 g CI in 360 ml of 0.5 M acetic acid using a blender (Ultra Turrax T18 Overhead Blended, IKA Works Inc., USA) at 15,000 rpm for 90 minutes at 4 °C, to a final concentration of 0.5% (w/v) CI. CI-HyA slurry was prepared by supplementing the CI slurry with 0.18 g of HyA and blending as described to yield a slurry with final concentration of 0.5% (w/v) CI and 0.05% (w/v) HyA. Slurries with a total collagen concentration of 0.5% (w/v) were then prepared using both CI and CII at a ratio of 1:1, type I:type II collagen (CI/II). Similarly, CI/II-HyA slurries were prepared with the same 1:1 type I:type II collagen ratio and final concentration of 0.5% (w/v) total collagen, in the presence of HyA 0.05% (w/v). Subsequently, 0.3 ml of each slurry was pipetted into a stainless-steel tray (internal dimensions: 9.5 mm diameter and 4 mm height) before freeze-drying (Virtis Genesis 25EL, Biopharma, UK) at a constant cooling rate of 1°C/min to a final temperature of -20°C, and drying at a pressure of 200 mTorr. Following this, the porous scaffolds were dehydrothermally (DHT) crosslinked in a vacuum oven (VacuCell, MMM, Germany) for 24 h at 0.05 bar pressure and 105 °C temperature. The scaffolds were then chemically crosslinked using a solution of 1-ethyl-3–(3-dimethylaminopropyl) carbodiimide (EDAC)/N-hydroxysuccinimide (NHS) (Sigma-Aldrich, Ireland), crosslinking at a ratio of 5:2 M, using a 6 mM concentration of EDAC per gram of collagen.

Table 1. Experimental collagen-based scaffolds manufactured and investigated for cartilage-like matrix regeneration. Scaffold biomaterials were composed of type I collagen (CI) and type II collagen (CII) at various ratios to prepare a series of scaffolds with a final collagen concentration of 0.5% (w/v), in the presence or absence of hyaluronic acid (HyA) at a concentration of 0.05% (w/v).

Scaffold type	CI% (w/v)	HyA% (w/v)	CII% (w/v)
CI	0.50%	/	/
CI/II	0.25%	/	0.25%
CI-HyA	0.50%	0.05%	/
CI/II-HyA	0.25%	0.05%	0.25%

2.2 Analysis of scaffold pore size and percentage porosity

Scaffold mean pore size and percentage porosity was determined histologically as previously described[25]. Briefly, scaffolds of 9.5 mm diameter and 4 mm height were prepared using 3 different batches of collagen slurry, before embedding in JB-4® glycolmethacrylate (Polysciences Europe, Germany) and longitudinally sectioning at various depths on a microtome (Leica RM 2255, Leica, Germany) to give 10 µm thick sections. These histological sections were subsequently stained using toluidine blue (Sigma-Aldrich, Ireland) which stains the collagen fibres blue. Digital images were captured at 10x magnification using an optical microscope (Eclipse 90i, Nikon, Japan) and a digital camera (DS Ri1, Nikon, Japan). Image J software was used to process the images. Pore size analysis was carried out on MATLAB (MathWorks Inc, USA) using a pore topology analyser developed in conjunction with the Sigmedia Research Group in the Electrical Engineering Department at Trinity College Dublin, Ireland[24]. The programme transformed the images into a binary format and calculated the average pore radii based on best-fit elliptical lengths. The porosity (%) of the scaffolds was measured according to Equation 1, where $\rho_{scaffold}$ is the apparent density of the scaffold measured by dividing the weight of the scaffold by the volume of the scaffold, and $\rho_{material}$ is the density of the material from which the scaffold was fabricated (1.3 mg/ml)[26].

Equation 1. Percentage porosity.

$$\textbf{Porosity}\ (\%) = \left(1 - \frac{\boldsymbol{\rho}\ \textbf{scaffold}}{\boldsymbol{\rho}\ \textbf{material}}\right) \times 100$$

2.3 Scanning electron microscope (SEM) analysis

To visualise the architecture of the dry, cell-free DHT crosslinked scaffolds, Scanning Electron Microscope (SEM) analysis was performed. Transverse sections across the minor axis of the scaffolds were collected and mounted onto metallic studs using carbon cement before sputter coating with a gold/palladium alloy using a current of 40 mA for 80 seconds (Cressington Scientific Instruments, UK). The sections were then imaged at several magnifications using a Zeiss Ultra Plus SEM at an accelerating voltage of 5 kV (Zeiss, Germany).

2.4 Analysis of scaffold mechanical properties

To determine the compressive elastic modulus of the cell-free scaffolds (n=6 per group) a uni-axial, unconfined compressive test was performed using a mechanical testing machine

(Z050, Zwick-Roell, Germany). Scaffolds were pre-hydrated in phosphate buffered saline (PBS) for 1 h prior to testing, with the amount of PBS being kept constant throughout the testing regime. The volume was enough to keep the scaffolds submerged. The scaffolds were then tested with a 5 N load and were kept immersed in PBS throughout the test. The analysis was conducted at a strain rate of 10% per minute. Stress was calculated from scaffold surface area and applied force, whilst strain was calculated from displacement of the scaffolds in relation to their original thickness. The compressive modulus was defined based on the slope of a linear fit to the stress–strain curve over 2%–5% strain.

2.5 Cell culture

Bone-marrow derived mesenchymal stem cells in monolayer

To obtain a sufficient quantity of rat mesenchymal stem cells (MSCs) for further experimentation, cells were first expanded in monolayer prior to seeding on the scaffolds. Bone marrow–derived MSCs were harvested from Wistar rats as previously described, under approval of the Royal College of Surgeons in Ireland Research Ethics Committee[27]. Cells were incubated in high-glucose Dulbecco's modified Eagle medium (DMEM) (Sigma-Aldrich, Ireland) supplemented with 10% fetal bovine serum (ThermoFisher Scientific, Ireland), 100 U/ml penicillin/streptomycin (ThermoFisher Scientific, Ireland), 1% L-glutamine (ThermoFisher Scientific, Ireland), 1% Glutamax (ThermoFisher Scientific, Ireland) and 1% non-essential amino acids (ThermoFisher Scientific, Ireland). Cells were passaged using trypsin ethylenediaminetetraacetic acid (EDTA, Sigma-Aldrich, Ireland) once confluent, before re-plating onto T-175 (175 cm^2 growth area) flasks under normoxic cell culture conditions (37 °C, 5% CO_2 and 21% O_2). Cells were cultured on the scaffolds at passage number 4.

Culture of bone-marrow derived mesenchymal stem cells on 3D scaffolds

Rat bone marrow-derived MSCs were detached from culture flasks via trypsinization. Cells were counted and re-suspended at a density of 5 x 10^5 cells per scaffold in a total volume of 100 µl. Scaffolds of 9.5 mm diameter and 4 mm height were pre-hydrated with 2mL per scaffold of PBS (Sigma-Aldrich, Ireland) for 15 minutes and placed in 24 well-plates. The excess of PBS was later removed prior the cell-seeding procedure on the scaffolds. The cell suspension was then added to the scaffolds, with 50 µl first pipetted onto one side of each scaffold, before incubating for 30 minutes (37 °C, 5% CO_2, 21% O_2) to allow initial cell attachment. Seeded scaffolds were subsequently turned over and the procedure repeated

on the other side. 2 ml of supplemented high-glucose DMEM growth medium was then added to each well and pre-cultured for 24 h. The high-glucose DMEM was later replaced with complete chondrogenic medium (CCM) containing 20 ng/ml human TGF-β3 (Prospec, Israel), or incomplete chondrogenic medium (ICM) prepared in the absence of human TGF-β3. The chondrogenic medium included 50 µg/ml ascorbic acid (ThermoFisher Scientific, Ireland), 40 µg/ml proline (ThermoFisher Scientific, Ireland), 100 nM dexamethasone (ThermoFisher Scientific, Ireland), 1X ITS (ThermoFisher Scientific, Ireland), and 0.11 mg/ml sodium pyruvate (ThermoFisher Scientific, Ireland). The cell-seeded scaffolds were incubated for 14 and 28 days, with media changed twice per week.

2.6 Cellular metabolic activity assay

To determine the metabolic activity of the cells within the scaffolds, an alamarblue assay (ThermoFisher Scientific, Ireland) was performed. Scaffolds (n=3 per group) were washed twice in PBS, and fresh ICM media containing 10% alamarblue viability reagent was added at 37 °C for 1 h. A spectrophotometer (Wallac 1420 Victor2 D, USA) with an excitation wavelength of 550 nm and an emission wavelength of 590 nm was used to read the resulting fluorescence level. ICM media containing 10% alamarblue was used as a blank sample, subtracted from the experimental readings to eliminate background fluorescence. The metabolic activity of the cells within the scaffolds was normalised at the respective time point to CI scaffolds after 14 and 28 days in CCM culture.

2.7 DNA quantification

To assess the DNA content in the scaffolds, a Quant-iT™ PicoGreen® dsDNA assay kit (Invitrogen, UK) was used as per the manufacturer's instructions. Scaffolds (n=3 per group) were washed in PBS and digested in a papain enzyme solution prepared with 0.5 M EDTA, cysteine-HCl and 1 mg/ml papain enzyme (Carica papaya, Sigma-Aldrich, Ireland) at 60 °C for 12 h. DNA concentration was determined using a standard curve, to give an indication of cell number.

2.8 Sulphated glycosaminoglycan (sGAG) quantification

To quantify the sulphated glycosaminoglycan (sGAG) content within the scaffolds, a Blyscan sulphated glycosaminoglycan assay kit (Biocolor Life Sciences, UK) was used. Scaffolds (n=3 per group) were washed in PBS before digesting in a solution prepared from papain enzyme solution containing 0.5 M EDTA, cysteine-HCl and 1 mg/ml papain enzyme (Carica

papaya, Sigma-Aldrich, Ireland) at 60 °C for 12 h. The Blyscan sulphated glycosaminoglycan assay was then performed as per the manufacturer's instructions. sGAG concentration was determined using a standard curve.

2.9 Histological analysis of cellular infiltration and sGAG distribution

Histological staining was performed to further evaluate cellular infiltration and sGAG distribution within the scaffolds. Scaffolds were fixed, embedded and transversally sectioned at various depths on a microtome (Leica RM 2255, Leica, Germany) to give 7 μm thick sections. These sections were subsequently mounted on Polysine^{TM} glass slides (Fisher-Scientific, Ireland), deparaffinised and hydrated before staining. The stains used in the histological analysis were haematoxylin (Sigma-Aldrich, Ireland), which stains the DNA- and RNA-rich cell nuclei blue; eosin (Sigma-Aldrich, Ireland), which stains the ECM pink; safranin-O (Sigma-Aldrich, Ireland), which stains sulphated GAGs red; and fast green, which provided a light counterstain for each sample. The sections were successively imaged at several magnifications using a Leica DMIL microscope (Leica Microsystems, Switzerland).

2.10 Gene expression analysis

To determine the expression of specific genetic markers associated with chondrogenic lineage, quantitative reverse transcriptase polymerase chain reaction (qRT-PCR) was conducted (Table 2). The total RNA was isolated from the scaffolds using a RNeasy kit (Qiagen, UK) as previously described[28]. RNA was then reverse transcribed to cDNA at a final concentration of 2.5 ng/μl using a QuantiTect reverse transcription kit (Qiagen, UK) on a thermal cycler (Mastercycler Personal, Eppendorf, UK). qRT-PCR reactions were run on a 7500 real-time PCR System (Applied Biosystems, UK) using a QuantiTect SYBR Green PCR kit (Qiagen, UK). The relative expression of mRNA was calculated using the delta-delta Ct ($\Delta\Delta$Ct) method, where delta Ct (ΔCt) is the value obtained by subtracting the cycle threshold value (Ct) of a house-keeping gene from the Ct value of target mRNAs: aggrecan (*ACAN*), collagen type II alpha 1 chain (*COL2A1*), collagen type I alpha 1 chain (*COL1A1*), runt-related transcription factor 2 (*RUNX2*) and collagen type X alpha 1 chain (*COL10A1*). The amount of target mRNA relative to the house-keeping gene was normalised to a calibrator sample to generate $\Delta\Delta$Ct. This was then converted to a fold increase in expression using the formula: Fold increase = $2^{-(\Delta\Delta Ct)}$. Glyceraldehyde 3-phospate dehydrogenase (*GAPDH*) was used as housekeeping gene.

Table 2. List of gene transcripts analysed by qRT-PCR. Qiagen QuantiTect validated primers were used to analyse the expression levels of target genes.

Target gene	Target gene reference	Catalogue code
Aggrecan (*ACAN*)	Rn_Acan_1_SG	QT00189518
Type II collagen alpha 1 chain (*COL2A1*)	Rn_Col2a1_1_SG	QT01084118
Type I collagen alpha 1 chain (*COL1A1*)	Rn_Col1a1_1_SG	QT00370622
Runt-related transcription factor 2 (*RUNX2*)	Rn_Runx2_1_SG	QT01300208
Type X collagen alpha 1 chain (*COL10A1*)	Rn_Col10a1_1_SG	QT00402479
Glyceraldehyde 3-phosphate dehydrogenase (*GAPDH*)	Rn_Gapdhs_1_SG	QT01082004

2.11 Statistical analysis

Results are expressed as mean ± standard deviation unless stated otherwise. Statistical analysis was carried out using GraphPad Prism software (version 9, GraphPad Software Inc.) using a general linear model one-way analysis of variance (ANOVA) with ordinary one-way ANOVA for single comparisons, or Tukey's post-hoc analysis for multiple comparisons. p-values less than or equal to 0.05 ($p \leq 0.05$) were considered statistically significant. * denotes $p \leq 0.05$, ** = $p \leq 0.01$, *** = $p \leq 0.001$ and **** = $p \leq 0.0001$.

3 Results

3.1 Incorporation of type II collagen increased the pore size of highly porous scaffolds with no detrimental impact on porosity

Scaffolds were first investigated for their morphological and architectural properties, which are essential to ensure cellular infiltration and viability for long periods in culture. Morphologically, pore size analysis revealed that the mean pore size of the scaffolds was significantly increased by the presence of CII (Fig. 1A, 1B). The composite CI/II scaffolds possessed the largest pores, measuring 159 ± 2.12 µm. These pores were significantly larger than those of the CI (122 ± 21.94 µm) and CI-HyA (113 ± 16.55 µm) scaffolds ($p \leq 0.05$). There was no statistical difference in mean pore size between CI/II and CI/II-HyA scaffolds which had a pore size of 155 ± 5.65 µm. CI/II-HyA scaffolds had larger pores than CI-HyA scaffolds ($p \leq 0.05$). There was no significant difference in pore dimension between the CI and CI-HyA scaffolds. Architecturally, all type I collagen-based scaffolds resulted in highly

porous structures, interconnected throughout the matrices, with a percentage porosity of 99% (Fig. 1C, 2).

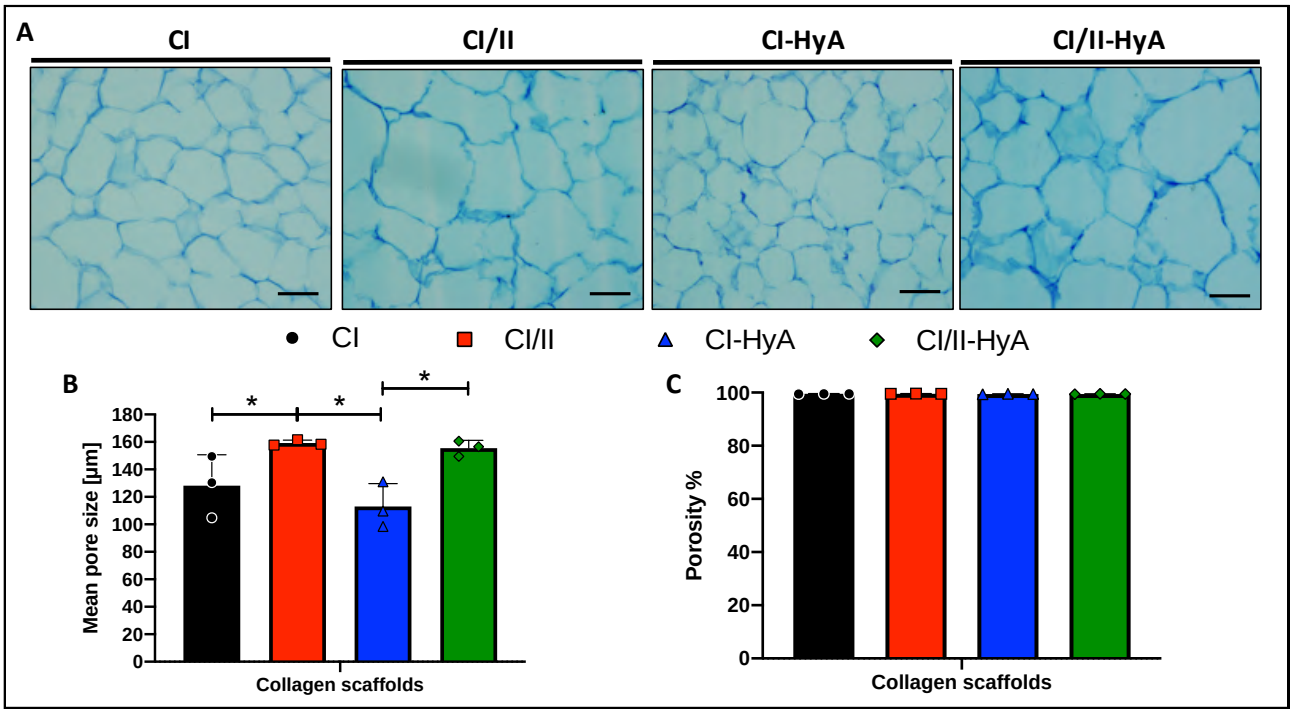

Figure 1. The incorporation of CII increased the pore size of highly interconnected porous scaffolds with no impact on porosity. Representative histological images of cell-free scaffolds stained with toluidine blue. Scale bar represents 100 µm length (**A**). The mean pore size (**B**) and percentage porosity (**C**) of cell-free scaffolds were determined. Data presented as mean ± SD, n=3. * denotes $p \leq 0.05$, ** = $p \leq 0.01$, *** = $p \leq 0.001$ and **** = $p \leq 0.0001$.

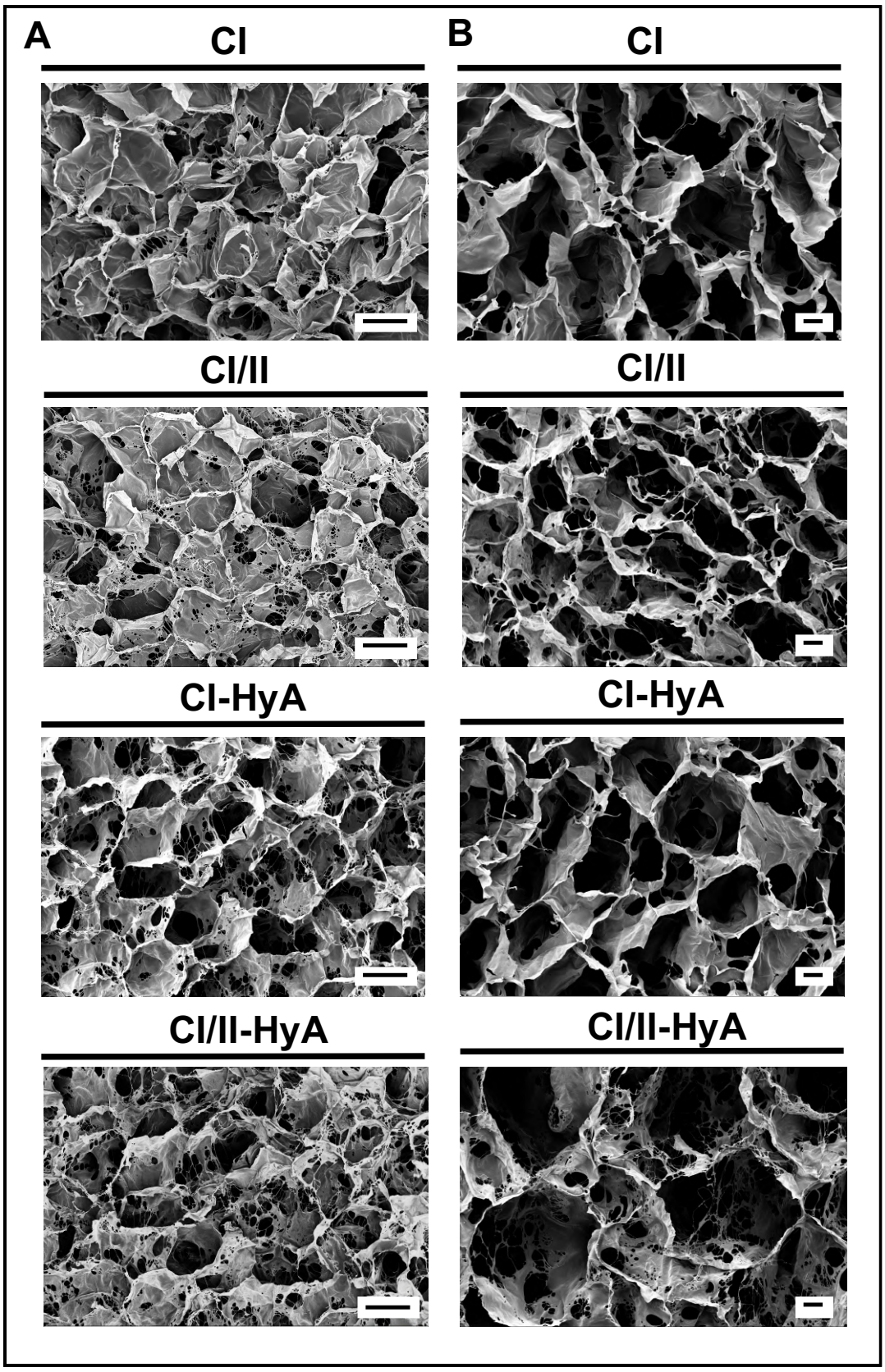

Figure 2. The incorporation of CII had no detrimental effect on the architecture of highly porous interconnected scaffolds. Representative SEM images at low (**A**) and high (**B**) magnification of the cell-free scaffolds at 5 kV. Scale bar = 100 μm for images in the left column (**A**); scale bar = 20 μm for images in the right column (**B**).

3.2 Type II collagen incorporation had no detrimental impact on scaffold compressive modulus

The effect of CII incorporation on the bulk compressive moduli of the scaffolds, a critical mechanical property to consider for applications in cartilage TE, was then investigated. Compressive tests revealed that the incorporation of CII had no detrimental impact on the bulk compressive moduli of cell-free scaffolds, which ranged between 1 and 0.4 kPa (Fig. 3). There was no statistical difference in the bulk compressive moduli between the different scaffold groups.

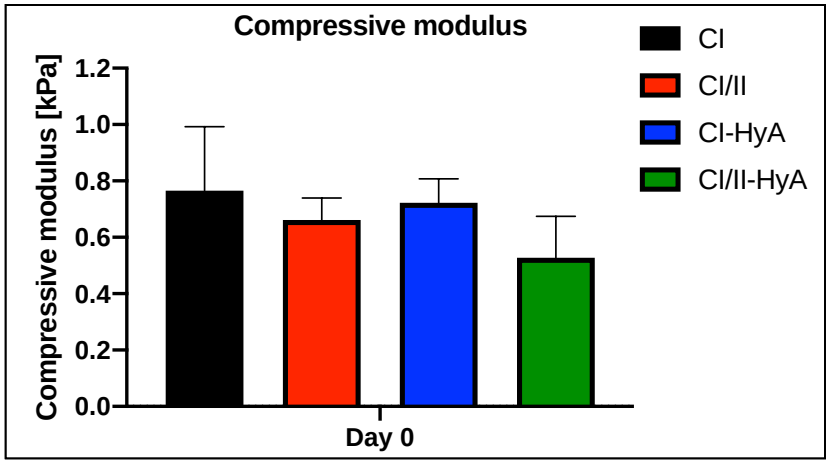

Figure 3. The incorporation of CII had no impact on the bulk compressive moduli of the cell-free scaffolds. The bulk compressive moduli of cell-free scaffolds were determined at day 0, after the cross-linking process. Data presented as mean ± SD, n=6.

3.3 Type II collagen in combination with hyaluronic acid increased cellular metabolism and growth

To assess biocompatibility, the capability of the scaffolds to sustain cellular viability and growth was investigated *in vitro*. The incorporation of CII in combination with HyA allowed CI/II-HyA scaffolds to sustain significantly increased cellular metabolic activity and growth compared to the other scaffold variants at day 28 (Fig. 4). The metabolic activity of the cells cultured was 5-fold higher for those in the CI/II-HyA scaffolds compared to the other groups at day 28 (CI $p \leq 0.001$; CI/II $p \leq 0.01$; CI-HyA $p \leq 0.001$) (Fig. 4A). The composite CI/II-HyA scaffolds also possessed the highest levels of DNA (1 µg/ml), representing a 2.5-fold increase in DNA levels compared to the other scaffold variants at day 28 ($p \leq 0.0001$) (Fig. 4B). DNA content increased between days 14 and 28 in all groups (CI $p \leq 0.0001$; CI/II $p \leq 0.001$; CI-HyA $p \leq 0.001$; CI/II-HyA $p \leq 0.0001$). At day 14 there was no statistical difference in cellular metabolic activity or DNA content per scaffold between groups. Moreover,

scaffolds cultured in incomplete chondrogenic medium (ICM) presented significantly lower levels of DNA content per scaffold compared to scaffolds cultured in complete chondrogenic medium (CCM) at day 28 (p≤0.0001).

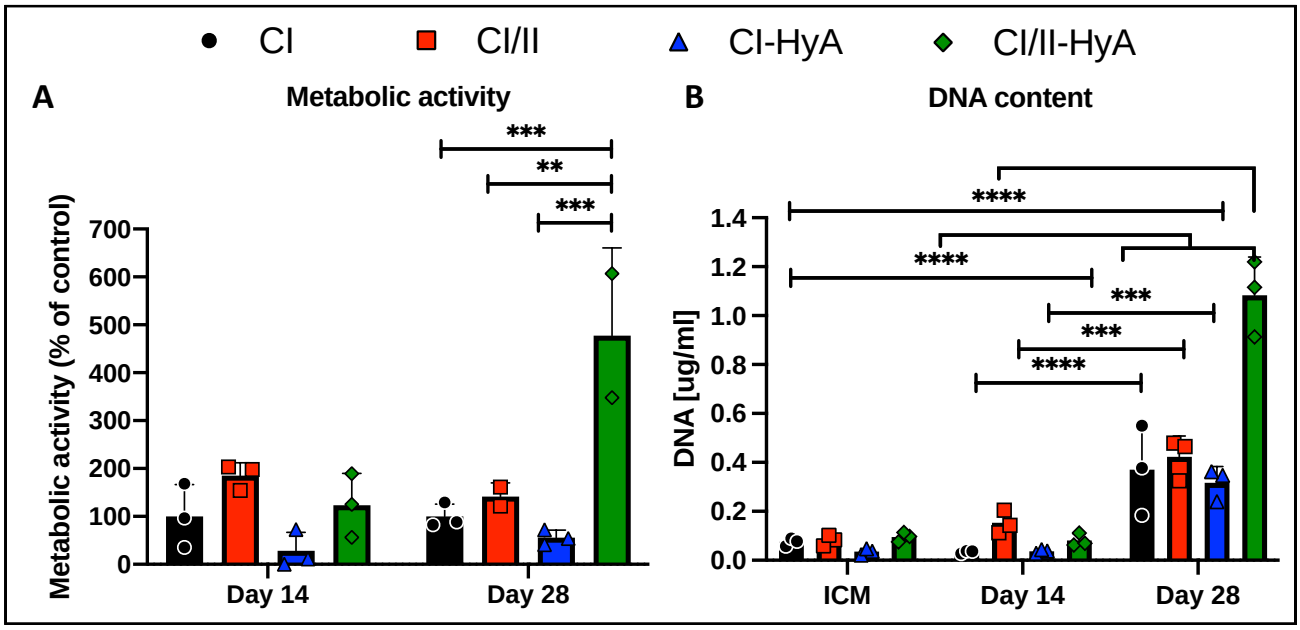

Figure 4. The incorporation of CII in combination with HyA improved MSC metabolic activity and growth at day 28. Cellular metabolic activity per scaffold was determined and normalised at the respective time point to CI scaffolds after 14 and 28 days in CCM culture (**A**). The DNA content per scaffold was determined after 28 days in ICM culture, and after 14 and 28 days in CCM culture (**B**). Data presented as mean ± SD, n=3 (unless indicated differently). * denotes p ≤ 0.05, ** = p ≤ 0.01, *** = p ≤ 0.001 and **** = p ≤ 0.0001.

3.4 Type II collagen in combination with hyaluronic acid increased the synthesis of sGAG by MSCs on the scaffolds

The ability of the scaffolds to direct MSC chondrogenesis and cartilage-like matrix formation *in vitro* was then evaluated. The incorporation of CII in combination with HyA allowed CI/II-HyA scaffolds to accumulate increased quantities of sulphated glycosaminoglycan (sGAG) per scaffold compared to the other scaffold variants at day 28 (Fig. 5A). CI/II-HyA scaffolds had the highest level of sGAG per scaffold at day 28 (57 µg/ml). This was significantly greater than all other groups at all time-points (p≤0.0001). In addition, the overall quantity of sGAG significantly increased between days 14 and 28 within each scaffold group (CI p≤0.0001; CI/II p≤0.001; CI-HyA p≤0.01; CI/II-HyA p≤0.0001). Normalised sGAG to DNA increased between days 14 and 28 in all scaffold variants (p≤0.0001). Moreover, scaffolds cultured in ICM presented significantly lower levels of sGAG deposition per scaffold and sGAG/DNA compared to scaffolds cultured in CCM at day 28 (p≤0.0001).

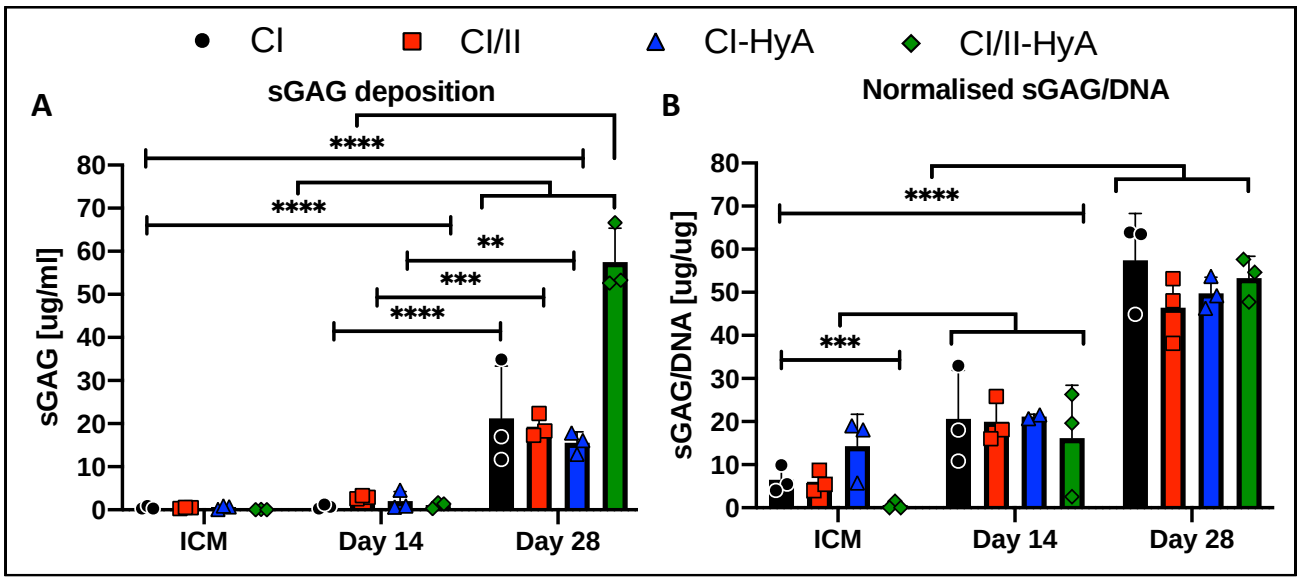

Figure 5. The incorporation of CII in combination with HyA increased the quantity of sGAG per scaffold at day 28. Overall sGAG per scaffold (**A**) and sGAG normalised to DNA content (**B**) respectively were determined after 28 days in ICM culture, and after 14 and 28 days in CCM culture. Data presented as mean ± SD, n=3. * denotes $p \leq 0.05$, ** = $p \leq 0.01$, *** = $p \leq 0.001$ and **** = $p \leq 0.0001$.

3.5 Type II collagen in combination with hyaluronic acid improved sGAG distribution throughout the scaffolds

To qualitatively assess the ability of the scaffolds to support rat MSC migration and cartilage-like matrix distribution (represented by sGAG) in the matrices, histological stains were analysed on cell-free and cell-seeded scaffolds. Haematoxylin and eosin staining revealed that all scaffold variants performed well, with an equal capability to direct efficacious cellular infiltration and migration throughout the matrices (Fig. 6). However, only the composite CI/II-HyA scaffold facilitated improved cartilage matrix distribution compared to the other scaffold variants as shown by safranin-O staining (Fig. 7). In particular, the incorporation of CII, in combination with HyA, allowed CI/II-HyA scaffolds to achieve more homogeneous sGAG distribution throughout the matrix compared to the other scaffold variants. In the composite CI/II and CI-HyA scaffolds, the majority of sGAG was found in the periphery of the scaffold, in contrast to the CI/II-HyA scaffolds where the sGAG was centrally distributed. Similarly in CI/II and CI-HyA scaffolds, the majority of the cells were distributed at the scaffold's periphery. CI scaffolds generally showed homogenous low-density cellular distribution in the scaffolds with no evidence of sGAG in the matrices. Overall, the composite CI/II-HyA scaffold induced more homogenous high-density cellular distribution throughout the scaffolds.

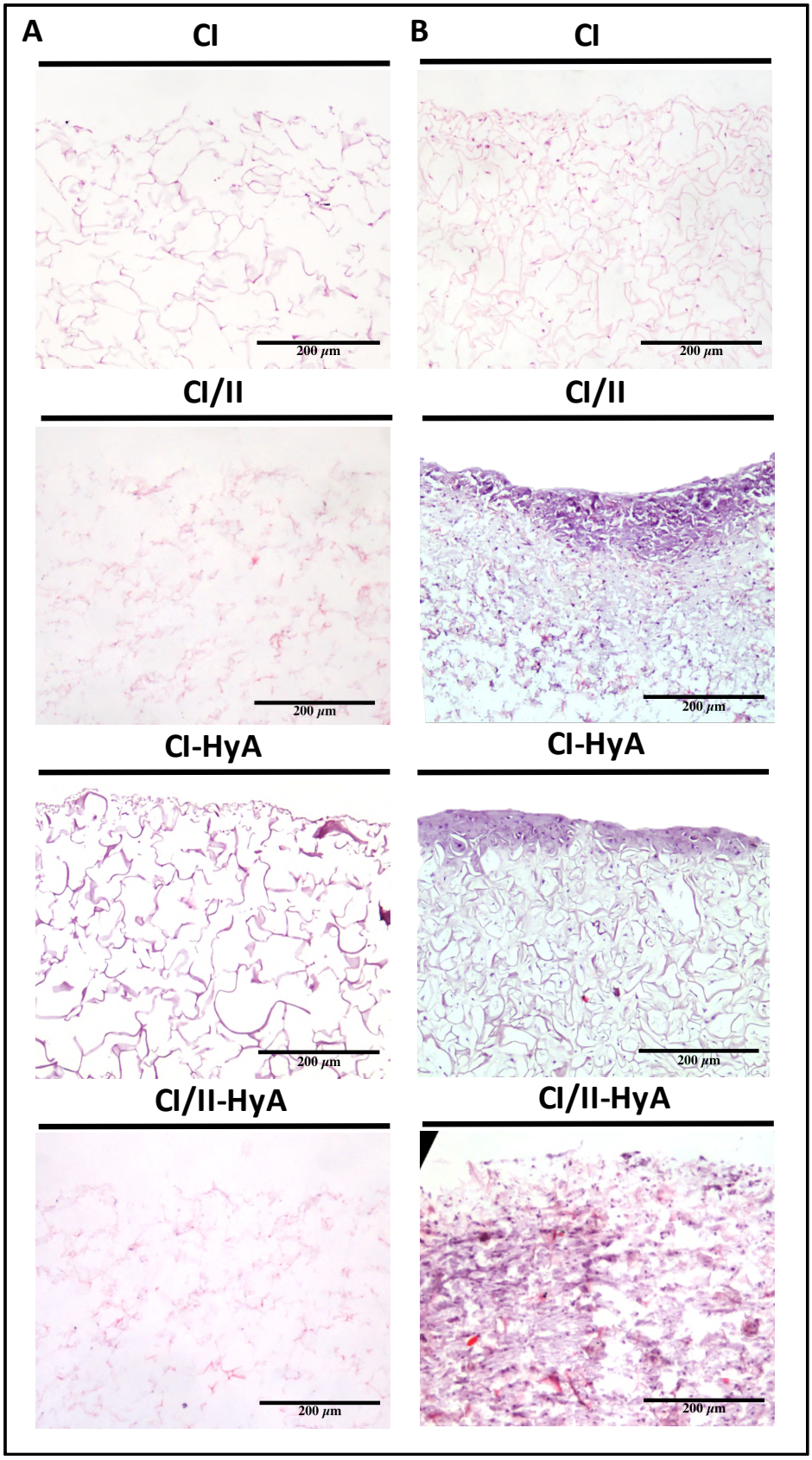

Figure 6. The incorporation of CII had no impact on the scaffolds' capacity to sustain cellular infiltration and migration. Representative histological images of cell-free (**A**) and cell-seeded (**B**) scaffolds stained with haematoxylin and eosin after 28 days in CCM culture. Scale bar represents 200 μm length.

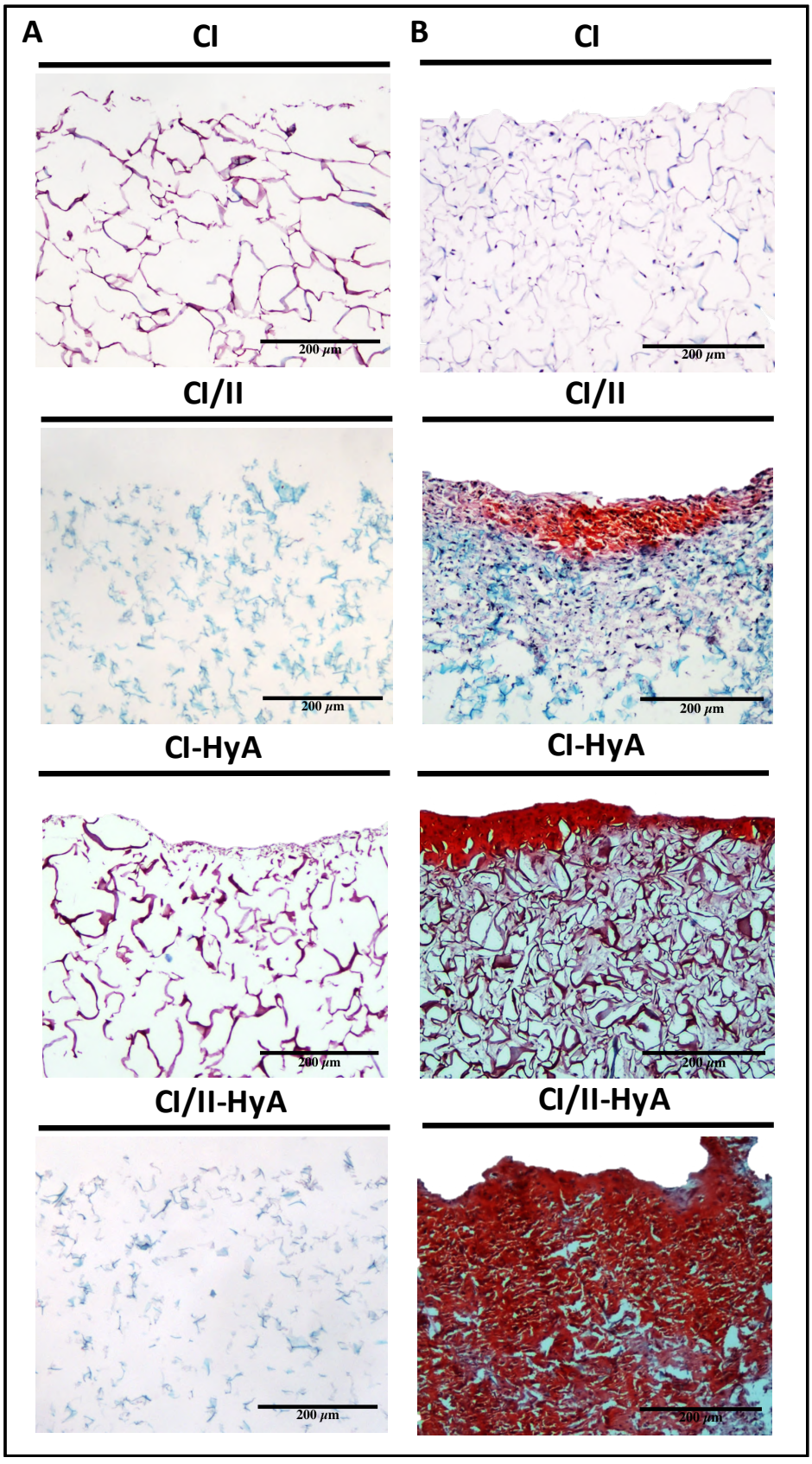

Figure 7. The incorporation of CII in combination with HyA improved sGAG distribution. Representative histological images of cell-free (**A**) and cell-seeded (**B**) scaffolds stained with haematoxylin, safranin-O and fast green after 28 days in CCM culture. Scale bar represents 200 μm length.

3.6 All scaffolds supported effective MSC chondrogenic gene expression, demonstrating potential for CI/II-HyA scaffolds to enhance chondrogenesis

The capability of the scaffolds to sustain rat MSC chondrogenic differentiation was then investigated by measuring the expression of specific genetic markers typically associated with effective MSC chondrogenesis and late-stage differentiation. All scaffold variants sustained *ACAN*, *COL2A1*, *COL1A1* and *COL10A1* gene expression by the MSCs at days 14 and 28 (Fig. 8). *ACAN* gene expression levels were significantly up-regulated at day 28 in the presence of CII ($p \leq 0.01$) (Fig. 8A). The incorporation of CII had no impact on *ACAN* gene expression at day 14. There was no statistical difference in *COL2A1*, *COL1A1*, *COL2A1/COL1A1*, *RUNX2* and *COL10A1* gene expression between the groups at days 14 or 28 (Fig. 2.8B-2.8F).

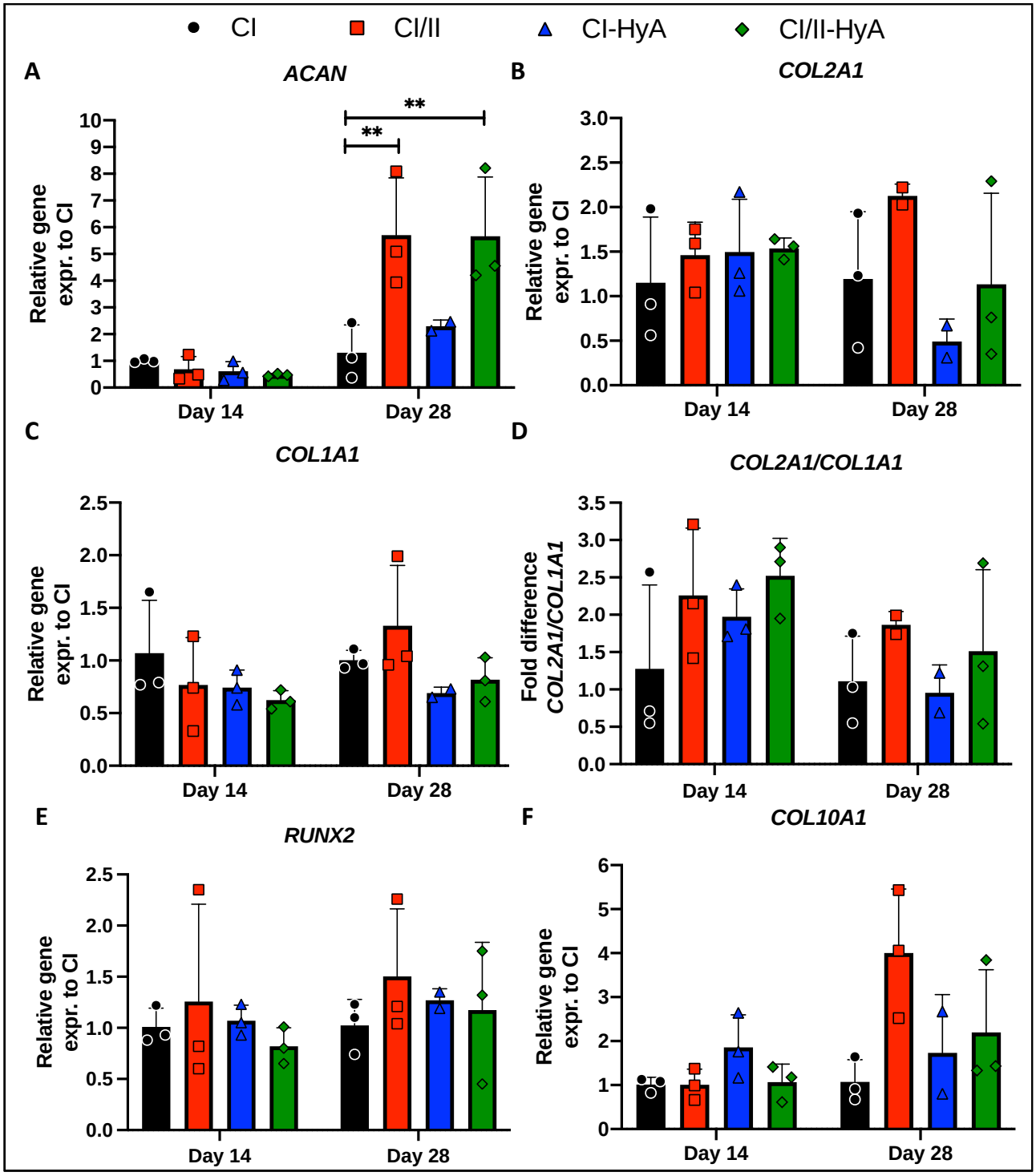

Figure 8. All collagen scaffolds supported the expression of genes associated with effective MSC chondrogenic differentiation. The expression of *ACAN* (**A**); *COL2A1* (**B**); *COL1A1* (**C**); *RUNX2* (**E**) and *COL10A1* (**F**) genes was determined after 14 and 28 days in CCM culture, normalised to *GAPDH* and converted to a fold increase in expression using the formula: Fold increase = 2-(ΔΔCt). The ratio between *COL2A1/COL1A1* expression is shown in (**D**). Data presented as mean ± SD, n=3 (unless indicated differently). * denotes p ≤ 0.05, ** = p ≤ 0.01, *** = p ≤ 0.001 and **** = p ≤ 0.0001.

4 Discussion

The overall aim of this study was to develop an innovative collagen-based scaffold for enhanced cartilage repair by incorporating type II collagen (CII) and/or hyaluronic acid (HyA) into a type I collagen (CI) framework. To this end, CII was incorporated into CI and/or HyA scaffold biomaterials previously designed by our laboratory for cartilage regeneration[10]. The newly developed CI/II and CI/II-HyA scaffolds exhibited highly porous interconnected structures with 99% porosity and similar mechanical properties to CI and CI-HyA scaffolds previously optimised. Although all four scaffold variants demonstrated early cartilaginous matrix deposition, the newly designed CI/II-HyA scaffold performed best, significantly improving the deposition and distribution of sulphate glycosaminoglycans (sGAG) *in vitro* by day 28. In addition, gene expression analysis revealed the potential for CII-containing scaffolds to further improve chondrogenesis, with up-regulated *ACAN* (a key articular cartilage ECM protein) expression at day 28 in the presence of CII. Taken together, the ability of CII and HyA to enhance MSC differentiation towards chondrogenesis and cartilage-like formation demonstrates that biomaterial composition plays a fundamental role in tissue engineering (TE) and can be manipulated to promote the synthesis of a hyaline-like cartilage ECM.

Architecturally, all collagen-based scaffolds presented uniform, highly interconnected porous matrices with approximately 99% porosity, comparable with previous data from our laboratory[10,26]. This high porosity ensures adequate diffusion of oxygen and nutrients within the constructs, which is essential to allow cellular infiltration and viability for long periods in culture[29,30,31]. Furthermore, the pore size of CI and CI-HyA scaffolds was also comparable to previous data from our laboratory[10,26]. However, the mean scaffold pore size was significantly increased in the presence of CII. Since all scaffold variants were manufactured using an identical freeze-drying protocol, the incorporation of CII within the colloid suspension altered it's freezing characteristics (i.e. colloid viscosity and consequent thermal conductivity), thus resulting in scaffolds with larger pores[24]. Previous studies have described minor differences in the molecular structure between CII and CI revealing the possibility that CII fibrils may also retain more water molecules than CI fibrils under the same conditions[32,33]. Therefore, it's possible that the incorporation of CII resulted in the formation of bigger ice crystals during the freezing process and consequently in scaffolds with larger pores[24].

Nevertheless, the dimension of the scaffolds' pores did not play a major role in directing successful MSC migration or cartilage matrix deposition. This is a crucial aspect to

understand since the dimension of the pores can impact MSC behaviour and responsiveness to migration and chondrogenesis[30,31,34]. Although CI/II and CI/II-HyA scaffolds had similar pore sizes, biochemical analysis revealed that the composite CI/II-HyA scaffolds presented higher levels of DNA content and improved sulphated glycosaminoglycans (sGAG) deposition/distribution compared to CI/II scaffolds. Additionally, full analysis revealed that CI/II scaffolds - which possessed larger pores than CI and CI-HyA - did not present a superior chondrogenic response, suggesting pore dimension did not regulate cellular infiltration and cartilage-like matrix deposition in the scaffolds, within the range investigated in this study. Similar results were previously obtained in our laboratory, where CI-HyA scaffolds with pores of 130 μm or 94 μm were equally capable of directing cellular migration and cartilage production throughout the matrices despite their different pore sizes[34]. To conclude, while the dimension of the scaffolds' pores is an important variable, we can assume that the biochemical composition of the scaffold plays a greater role in directing effective MSC chondrogenesis.

In cell-free scaffolds, the incorporation of CII had no impact on bulk compressive modulus - a critical mechanical property to consider in cartilage TE[29]. This result was somewhat unexpected given the well-known deficiencies in the mechanical properties of CII-based biomaterials, which limits their application in cartilage TE[35]. Although CII and CI share a similar chemical nature, and both can form strong fibrils in the human body, CII fibrils are typically smaller in dimension with inferior mechanical properties including long-term resistance to stress-strain variation[36,37]. Indeed, previous studies have confirmed inferior compressive moduli of hydrogels made of CII compared to CI-only hydrogels[38]. Here, it may be possible that the cross-linking procedures applied during the scaffold fabrication process might have mitigated the poor mechanical properties of CII, reinforcing it, as previously described[39]. Another possible explanation may be the co-presence of mechanically stronger CI enhanced or somewhat masked the poorer mechanical properties of CI and CI-HyA scaffolds incorporating CII. Ultimately, the similar compressive moduli of all the scaffolds evaluated demonstrates that scaffold biochemical composition, not scaffold mechanical properties, most strongly influenced MSC chondrogenic potential and cartilage regeneration capacity in this study.

Biologically, the incorporation of CII in combination with HyA led to improved MSC viability and growth by day 28 compared to other scaffold variants. This beneficial effect of CII in

tandem with HyA has not previously been described in the literature. Previous studies have evaluated CII's individual capacity to sustain MSC or articular chondrocyte growth, revealing a favourable influence when it is incorporated into 2D or 3D matrices[15,40]. Interestingly, it has been reported in other studies that when CII is combined with other cartilaginous ECM components such as CI or chondroitin sulphate, there is no further improvement in cellular growth[38,40,41]. For instance, CI hydrogels combined with CII and cultured with human bone marrow-derived MSCs sustained cellular viability and proliferation equivalent to, but not better than that of CI-only hydrogels (a result confirmed by this study). This work therefore highlights a major and previously unseen co-operative role between CII and HyA (when combined within 3D collagen-based scaffolds) that improved MSC viability and growth *in vitro*.

Another very notable beneficial effect observed when combining CII with HyA was the improved and more robust MSC-mediated chondrogenic response. Although all collagen-based scaffolds performed well *in vitro*, the composite CI/II-HyA scaffolds promoted significantly enhanced cartilage-like matrix deposition and distribution compared to the other scaffold variants. The composite CI/II-HyA scaffolds yielded 3-fold higher levels of sGAG per scaffold. Comparing these findings with other studies supports the hypothesis that CII exerts its effect by supporting a greater overall synthesis of new cartilage-like matrix in the scaffolds, rather than increasing the rate of cartilage synthesis by the cells[15,40]. Thus, CII appears to enhance the synthesis of new cartilage-like matrix by increasing cellular proliferation in the matrices. Of note, it has been shown that the incorporation of CII into chitosan hydrogels can promote greater sGAG deposition by rabbit articular chondrocytes in parallel with increased levels of DNA content, compared to chitosan hydrogels incorporating chondroitin sulphate[15]. These outcomes correlate with the results in this work showing higher levels of DNA content per scaffold, matching greater sGAG deposition and distribution in the matrices. Taken together, although this work highlights a major and essential co-operative role between CII and HyA when incorporated into collagen-based scaffolds, a deeper understanding of the cellular and molecular mechanisms governing this effect of CII with HyA is needed, and thus remains an important area of interest in TE.

Additionally, this study has proven that all scaffolds supported successful MSC chondrogenic differentiation, with some potential for CI/II-HyA scaffolds to enhance chondrogenesis. In particular, *ACAN* expression levels were significantly up-regulated at day 28 in the presence

of CII. While there are no equivalent studies to corroborate these results, previous studies have associated significant down-regulation of *ACAN* gene expression with late-stage MSC chondrogenesis and early hypertrophy[42,43]. Therefore, although caution should be taken in assessing the effect of CII, the increased expression of *ACAN* genes observed at this late time-point in culture may indicate that chondrocytes are not tending towards late-stage differentiation and hypertrophy. This hypothesis is in agreement with a recent study by Lian C. *et al.* which has proven CII's ability to promote decreased expression of type X collagen (Col10), a specific protein typically associated with late-stage chondrogenesis and calcified cartilage[17]. Future research might further evaluate the capability of CII biomaterials to control and modulate MSC differentiation to endochondral bone *in vitro*.

5 Conclusion

The combination of type II collagen (CII) and hyaluronic acid (HyA) resulted in the development of a CII containing scaffold with improved chondrogenic benefits, with no impact on the essential mechanical properties of the scaffold. The biochemical nature of these components can play a significant role in enhancing cellular growth and cartilage-like deposition/distribution. In summary, these findings make CI/II-HyA an excellent scaffold for further investigation for simple and effective "off-the-shelf" application in patients, with promise to direct enhanced repair of focal cartilage defects.

Author contributions

Conceptualization, Claudio Intini, John P. Gleeson and Fergal J. O'Brien; investigation, Claudio Intini, Mark Lemoine and Tom Hodgkinson; writing-review and editing, Claudio Intini, Mark Lemoine, Tom Hodgkinson, Sarah Casey, John P. Gleeson and Fergal J. O'Brien; funding acquisition, John P. Gleeson and Fergal J. O'Brien. All authors have read and agreed to the published version of the manuscript.

Conflicts of interest

The authors declare no conflict of interest.

Acknowledgements

This work was financially supported by the European Union's Horizon 2020 research and innovation programme under Marie Sklodowska-Curie grant agreement No 721432, and by the European Research Council (ERC) Advanced Grant n°788753 (ReCaP).

Bibliography

1. O'Brien, F. J. Biomaterials & scaffolds Every day thousands of surgical procedures are performed to replace. *Mater. Today* **14**, 88–95 (2011).
2. Ma, P. X. Biomimetic materials for tissue engineering. *Adv. Drug Deliv. Rev.* **60**, 184–198 (2008).
3. Howard, D., Buttery, L. D., Shakesheff, K. M. & Roberts, S. J. Tissue engineering: strategies, stem cells and scaffolds. *J. Anat.* **213**, 66–72 (2008).
4. Pina, S. *et al.* Scaffolding Strategies for Tissue Engineering and Regenerative Medicine Applications. *Materials (Basel).* **12**, 1824 (2019).
5. Dong, C. & Lv, Y. Application of Collagen Scaffold in Tissue Engineering: Recent Advances and New Perspectives. *Polymers (Basel).* **8**, 42 (2016).
6. Irawan, V., Sung, T.-C., Higuchi, A. & Ikoma, T. Collagen Scaffolds in Cartilage Tissue Engineering and Relevant Approaches for Future Development. *Tissue Eng. Regen. Med.* **15**, 673–697 (2018).
7. Tallawi, M. *et al.* Strategies for the chemical and biological functionalization of scaffolds for cardiac tissue engineering: a review. *J. R. Soc. Interface* **12**, 20150254 (2015).
8. Rappu, P., Salo, A. M., Myllyharju, J. & Heino, J. Role of prolyl hydroxylation in the molecular interactions of collagens. *Essays Biochem.* **63**, 325–335 (2019).
9. Loeser, R. F. Integrins and chondrocyte–matrix interactions in articular cartilage. *Matrix Biol.* **39**, 11–16 (2014).
10. Matsiko, A., Levingstone, T. J., O'Brien, F. J. & Gleeson, J. P. Addition of hyaluronic acid improves cellular infiltration and promotes early-stage chondrogenesis in a collagen-based scaffold for cartilage tissue engineering. *J. Mech. Behav. Biomed. Mater.* **11**, 41–52 (2012).
11. Blumbach, K. *et al.* Combined role of type IX collagen and cartilage oligomeric matrix protein in cartilage matrix assembly: Cartilage oligomeric matrix protein counteracts type IX collagen induced limitation of cartilage collagen fibril growth in mouse chondrocyt. *Arthritis Rheum.* **60**, 3676–3685 (2009).
12. Firner, S. *et al.* Extracellular Distribution of Collagen II and Perifibrillar Adapter Proteins in Healthy and Osteoarthritic Human Knee Joint Cartilage. *J. Histochem. Cytochem.* **65**, 593–606 (2017).
13. Goldring, M. *et al.* Roles of inflammatory and anabolic cytokines in cartilage metabolism: signals and multiple effectors converge upon MMP-13 regulation in

osteoarthritis. *Eur. Cells Mater.* **21**, 202–220 (2011).

14. Xin, W., Heilig, J., Paulsson, M. & Zaucke, F. Collagen II regulates chondroycte integrin expression profile and differentiation. *Connect. Tissue Res.* **56**, 307–314 (2015).
15. Choi, B., Kim, S., Lin, B., Wu, B. M. & Lee, M. Cartilaginous Extracellular Matrix-Modified Chitosan Hydrogels for Cartilage Tissue Engineering. *ACS Appl. Mater. Interfaces* **6**, 20110–20121 (2014).
16. Chang, K.-Y., Hung, L.-H., Chu, I.-M., Ko, C.-S. & Lee, Y.-D. The application of type II collagen and chondroitin sulfate grafted PCL porous scaffold in cartilage tissue engineering. *J. Biomed. Mater. Res. Part A* **92A**, 712–723 (2010).
17. Lian, C. *et al.* Collagen type II suppresses articular chondrocyte hypertrophy and osteoarthritis progression by promoting integrin β1−SMAD1 interaction. *Bone Res.* **7**, 8 (2019).
18. Lu, Z., Doulabi, B. Z., Huang, C., Bank, R. A. & Helder, M. N. Collagen Type II Enhances Chondrogenesis in Adipose Tissue–Derived Stem Cells by Affecting Cell Shape. *Tissue Eng. Part A* **16**, 81–90 (2010).
19. Chen, S., Fu, P., Cong, R., Wu, H. & Pei, M. Strategies to minimize hypertrophy in cartilage engineering and regeneration. *Genes Dis.* **2**, 76–95 (2015).
20. Levingstone, T. J., Matsiko, A., Dickson, G. R., O'Brien, F. J. & Gleeson, J. P. A biomimetic multi-layered collagen-based scaffold for osteochondral repair. *Acta Biomater.* **10**, 1996–2004 (2014).
21. Levingstone, T. J. *et al.* Multi-layered collagen-based scaffolds for osteochondral defect repair in rabbits. *Acta Biomater.* **32**, 149–160 (2016).
22. Levingstone, T. J. *et al.* Cell-free multi-layered collagen-based scaffolds demonstrate layer specific regeneration of functional osteochondral tissue in caprine joints. *Biomaterials* **87**, 69–81 (2016).
23. Franklyn-Miller, A. O. and their role in cartilage injury. [cited 2020 A. 28]. A. from: https://soundcloud.com/sports-surgery-clinic/ professor-cathal-moran-podcast-16-04-2020-1242.
24. Haugh, M. G., Murphy, C. M. & O'Brien, F. J. Novel Freeze-Drying Methods to Produce a Range of Collagen–Glycosaminoglycan Scaffolds with Tailored Mean Pore Sizes. *Tissue Eng. Part C Methods* **16**, 887–894 (2010).
25. O'Brien, F.J. Influence of freezing rate on pore structure in freeze-dried collagen-GAG scaffolds. *Biomaterials* **25**, 1077–1086 (2004).

26. Raftery, R. M. *et al.* Multifunctional biomaterials from the sea: Assessing the effects of chitosan incorporation into collagen scaffolds on mechanical and biological functionality. *Acta Biomater.* **43**, 160–169 (2016).
27. Raftery, R. M., Tierney, E. G., Curtin, C. M., Cryan, S.-A. & O'Brien, F. J. Development of a gene-activated scaffold platform for tissue engineering applications using chitosan-pDNA nanoparticles on collagen-based scaffolds. *J. Control. Release* **210**, 84–94 (2015).
28. Duffy, G. *et al.* Towards in vitro vascularisation of collagen-GAG scaffolds. *Eur. Cells Mater.* **21**, 15–30 (2011).
29. O'Brien, F. J. Biomaterials & scaffolds for tissue engineering. *Mater. Today* **14**, 88–95 (2011).
30. Murphy, C. M., Duffy, G. P., Schindeler, A. & O'Brien, F. J. Effect of collagen-glycosaminoglycan scaffold pore size on matrix mineralization and cellular behavior in different cell types. *J. Biomed. Mater. Res. Part A* **104**, 291–304 (2016).
31. Murphy, C. M., Haugh, M. G. & O'Brien, F. J. The effect of mean pore size on cell attachment, proliferation and migration in collagen–glycosaminoglycan scaffolds for bone tissue engineering. *Biomaterials* **31**, 461–466 (2010).
32. Grynpas, M. D., Eyre, D. R. & Kirschner, D. A. Collagen type II differs from type I in native molecular packing. *Biochim. Biophys. Acta - Protein Struct.* **626**, 346–355 (1980).
33. Antipova, O. & Orgel, J. P. R. O. In Situ D-periodic Molecular Structure of Type II Collagen. *J. Biol. Chem.* **285**, 7087–7096 (2010).
34. Matsiko, A., Gleeson, J. P. & O'Brien, F. J. Scaffold Mean Pore Size Influences Mesenchymal Stem Cell Chondrogenic Differentiation and Matrix Deposition. *Tissue Eng. Part A* **21**, 486–497 (2015).
35. Yang, K. *et al.* Photo-crosslinked mono-component type II collagen hydrogel as a matrix to induce chondrogenic differentiation of bone marrow mesenchymal stem cells. *J. Mater. Chem. B* **5**, 8707–8718 (2017).
36. Shoulders, M. D. & Raines, R. T. Collagen Structure and Stability. *Annu. Rev. Biochem.* **78**, 929–958 (2009).
37. Shen, Z. L., Dodge, M. R., Kahn, H., Ballarini, R. & Eppell, S. J. Stress-Strain Experiments on Individual Collagen Fibrils. *Biophys. J.* **95**, 3956–3963 (2008).
38. Tamaddon, M. *et al.* Monomeric, porous type II collagen scaffolds promote chondrogenic differentiation of human bone marrow mesenchymal stem cells in vitro.

Sci. Rep. **7**, 43519 (2017).

39. Tierney, C. M. *et al.* The effects of collagen concentration and crosslink density on the biological, structural and mechanical properties of collagen-GAG scaffolds for bone tissue engineering. *J. Mech. Behav. Biomed. Mater.* **2**, 202–209 (2009).
40. Cao, H. & Xu, S.-Y. EDC/NHS-crosslinked type II collagen-chondroitin sulfate scaffold: characterization and in vitro evaluation. *J. Mater. Sci. Mater. Med.* **19**, 567–575 (2008).
41. Kilmer, C. E. *et al.* Collagen Type I and II Blend Hydrogel with Autologous Mesenchymal Stem Cells as a Scaffold for Articular Cartilage Defect Repair. *ACS Biomater. Sci. Eng.* **6**, 3464–3476 (2020).
42. Li, I. M. H. *et al.* Differential tissue specific, temporal and spatial expression patterns of the Aggrecan gene is modulated by independent enhancer elements. *Sci. Rep.* **8**, 950 (2018).
43. Takimoto, A. *et al.* Differential transactivation of the upstream aggrecan enhancer regulated by PAX1/9 depends on SOX9-driven transactivation. *Sci. Rep.* **9**, 4605 (2019).